Effect of Design Variables on Irreversible Permanent Magnet Demagnetization in Flux-Reversal Machine

Heung-Kyo Shin, *Tae Heoung Kim, Hwi-Beom Shin, and Soon-Young Lee

Department of Electrical Engineering, Engineering Research Institute, Gyeongsang National University, Jinju, Gyeongnam 660-701, Korea

*Corresponding Author (Phone: 82-55-751-5349   Fax: 82-55-759-2723   E-mail: ktheoung@gnu.ac.kr)

Abstract— **The large demagnetizing currents in Flux-Reversal Machine (FRM) are generated by the short-circuited of stator windings and the fault of a drive circuit. So, irreversible magnet demagnetization occurs due to the external demagnetizing field by these currents.**

In this paper, we deal with the effect of design variables on irreversible magnet demagnetization in the FRM using two-dimensional finite-element method (2D FEM). The nonlinear analysis of a permanent magnet is added to 2D FEM to consider irreversible demagnetization. As a result, it is shown that magnet thickness and rotor teeth width are the most important geometrical dimensions of the FRM in terms of irreversible magnet demagnetization.

I. INTRODUCTION

Research interest in the switched reluctance motor (SRM) has grown significantly in recent years because of their apparent advantages such as simple construction, fault tolerance and mechanical robustness. On the other hand, some of their limitations (such as excitation penalty, control complexity, noise and vibration) have prompted research into the incorporation of permanent magnets into the basic SRM structure. One of the new topologies proposed recently is a FRM. The FRM is a new brushless doubly salient permanent magnet machine proposed with the same aim of combining the advantages of the SRM and the permanent magnet brushless DC motor (BLDCM). The permanent magnet flux linkage in the stator phase concentrated coils reverses polarity with the rotor traveling. Its simple structure makes it cost effective and suitable for mass production. It has low self and mutual inductances, hence a low electrical time constant and high fault tolerance [1][2].

Because the permanent magnets are on the teeth surface of stator, the FRM is likely to face on irreversible magnet demagnetization caused by the large demagnetizing currents. These currents are generated by the short-circuited stator windings and the fault of a drive circuit. The irreversible magnet demagnetization can cause deterioration of motor performance such as torque ability [3][4]. Therefore, it should be considered in the design of the FRM.

In this paper, we deal with the effect of design variables on irreversible magnet demagnetization in the FRM using 2D FEM. The nonlinear characteristic of the permanent magnet is considered as well as that of a magnetic core on each B-H curve. From the analysis results, the most important geometrical dimensions are suggested in terms of irreversible magnet demagnetization.

II. ANALYSIS MODEL

Fig. 1 shows the prototype FRM. It has a six-pole stator and eight-pole variable reluctance rotor. The permanent magnet material is sintered Nd-Fe-B. The air gap was designed to be 0.5 mm to obtain a reasonable permeance coefficient value. The stator and the rotor pole arcs were designed to be 45° and 22.5° respectively. Table I summarizes the important FRM design specifications.
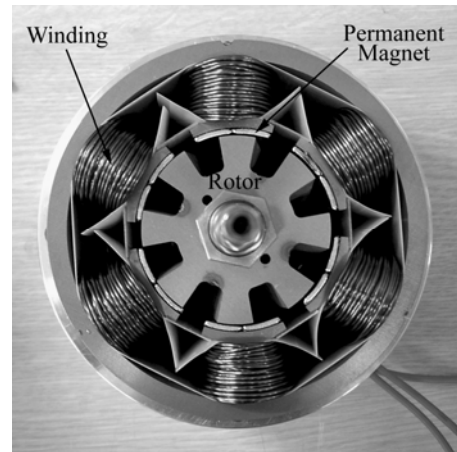
Fig. 1. Configuration of prototype FRM.

TABLE I
SPECIFICATIONS OF THE PROTOTYPE FRM

Section	Item	Value	(Unit)
Stator	Number of phases	3	
	Number of slots	6	
	Outer diameter	112	(mm)
	Stack width	60	(mm)
	Number of turns / phase / pole	96	(turns)
Rotor	Number of poles	8	
	Outer diameter	55	(mm)
	Pole length	10	(mm)
Magnet	Material	Nd-Fe-B	
	Residual flux density (Br)	1.15	(T)
Air gap	Mechanical air gap	0.5	(mm)

III. FINITE ELEMENT FORMULATIONS

A. Discretization

The two-dimensional governing equation for the FRM is expressed in magnetic vector potential by the following [5]:

$$\frac{\partial}{\partial x}\left(\frac{1}{\mu}\frac{\partial A_z}{\partial x}\right) + \frac{\partial}{\partial y}\left(\frac{1}{\mu}\frac{\partial A_z}{\partial y}\right) = -J_0 - \frac{1}{\mu_0}\left(\frac{\partial M_y}{\partial x} - \frac{\partial M_x}{\partial y}\right) \quad (1)$$

where

A_z : Z component of magnetic vector potential

J_0 : Current density

M : Magnetization of the permanent magnet

Applying the Galerkin method to (1), we can obtain the finite element equation in a first order triangular element as follows:

$$I_{ie} = \int_{Se} \frac{1}{\mu} \sum_{j=1}^{3} \left(\frac{\partial N_{ie}}{\partial x}\frac{\partial N_{je}}{\partial x} + \frac{\partial N_{ie}}{\partial y}\frac{\partial N_{je}}{\partial y} \right) A_{je} dxdy$$

$$- \int_{Se} \frac{1}{\mu_0}\left(M_x^e \frac{\partial N_{ie}}{\partial y} - M_y^e \frac{\partial N_{ie}}{\partial x} \right) dxdy - \int_{Se} J_0 N_{ie} dxdy \quad (2)$$

where N stands for shape function.

B. Nonlinear Analysis of a Permanent Magnet

In order to perform the nonlinear calculation of a permanent magnet, we use the approximate equation for magnetization M of a magnet. Fig. 2(a) shows a typical demagnetization curve of permanent magnet materials. From this graph, we can find $H = f(B)$. Then, the approximate equation for magnetization M is derived as follows:

$$M = B - \mu_0 H = B - \mu_0 f(B) = h(B) \quad (3)$$

where M is magnetization of a permanent magnet and μ_0 is permeability. Equation (3) means that the magnetization M of magnet is a function of flux density B. Fig. 2(b) shows the $M - B$ curve of permanent magnet.

(a) Demagnetization curve

(b) M-B curve

Fig. 2. Characteristic curve of permanent magnet.

Applying the Newton-Raphson method to (2), we can obtain the following equation to be related with equivalent magnetic current density J_{mi}.

$$\frac{\partial J_{mi}^e}{\partial A_{je}} = \frac{v_0}{4\Delta^e}\left(\frac{\partial M_x^e}{\partial B_x} d_{ie} d_{je} + \frac{\partial M_y^e}{\partial B_y} c_{ie} c_{je} \right) \quad (4)$$

where Δ^e is the area of an element and c and d are the coefficients that are related with the coordinate.

IV. ANALYSIS RESULTS AND DISCUSSION

Fig. 2(a) also shows the procedure of demagnetization. When operating point P_1 moves to P_2 due to the external demagnetization field, the residual flux density B_r is decreased to $B_r^`$, and irreversible magnet demagnetization occurs. As a result, the magnetization of the magnet is also decreased.

Fig. 3 shows the 1/2 cross-sectional configuration of the analysis model. It is possible to analyze only a 1/2 model by periodic boundary condition. The geometrical design variables and the mechanical angle of the magnet position are indicated in order to investigate magnet demagnetization.

Fig. 3. Cross-sectional configuration of the analysis model.

Fig. 4 shows the back electromotive force (Back-EMF) according to magnet thickness. The Back-EMF decreases as the magnet thickness increases. When the

magnet thickness is 1mm, this prototype FRM has an optimum value from the Back-EMF maximum point of view. However, we selected 2mm for the prototype FRM to consider the irreversible permanent magnet demagnetization. The cogging torque was also compared as shown in Fig. 5.
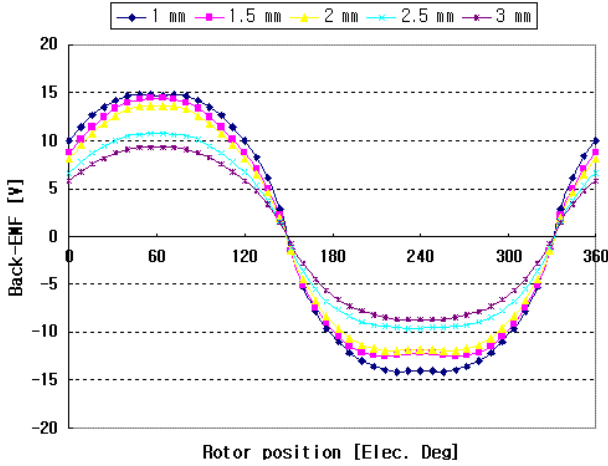
Fig. 8 shows the effect of rotor teeth width *Rtw* on demagnetization when the MMF is 2100 Ampere-turns. From the figure, the demagnetization increases as the teeth surface width, *Rtw*, decreases. This is due to the concentrated external demagnetization field on the magnet.
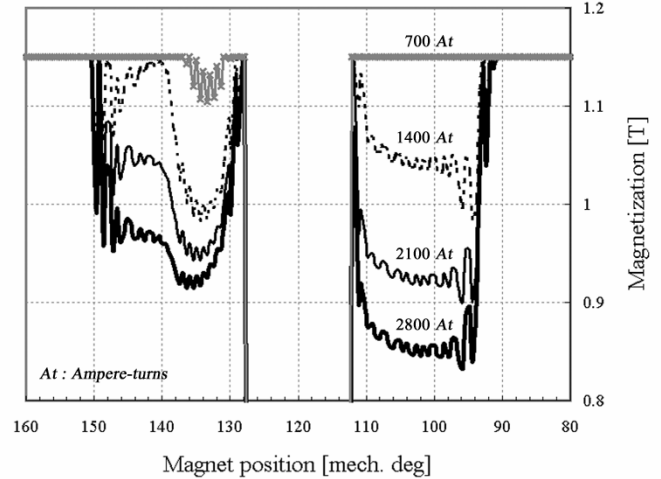

Fig. 4. Back-EMF waveforms according to magnet thickness.

Fig. 6. Effects of MMF on demagnetization.

Fig. 5. Cogging torque according to magnet thickness.
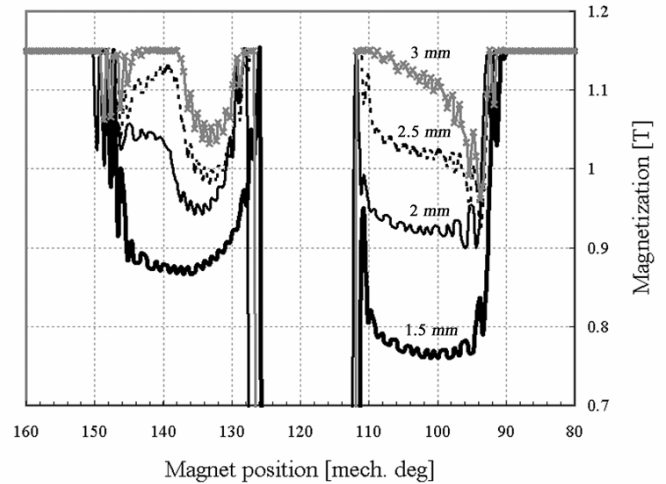
Fig. 7. Effects of magnet thickness L_m on demagnetization.

Fig. 6 shows the effect of magneto-motive force [MMF] on demagnetization when two phases (b and c) are energized. The reason why only two phases are energized is that the FRM is driven by alternating pulses of rectangular currents of 120-degree base. The x-axis is the magnet position while the y-axis is the magnetization of a magnet. The magnet has initial 1.15T magnetization before demagnetization. However, it is decreased after demagnetization as shown in Fig. 2(a). From Fig. 6, we can see that the magnet demagnetization becomes larger as the MMF increases.

Fig. 7 shows the effect of magnet thickness L_m on demagnetization when the MMF is 2100 Ampere-turns. The demagnetization decreases as the magnet thickness increases. This is because the permeance coefficient is higher and the external demagnetization field is smaller according to Ampere's Law. So, it is very important to select a proper value of the magnet thickness in design of a FRM.
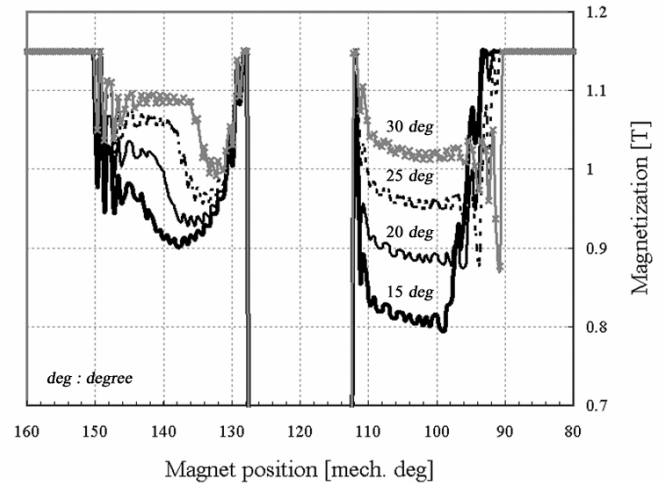

Fig. 8. Effects of rotor teeth width Rtw on demagnetization.

Fig. 9 and 10 show the magnetization distribution and flux vectors of the magnet when MMF is 700 and 2100 Ampere-turns, respectively. We can see that the local demagnetization is generated in the magnet by the external demagnetization field.
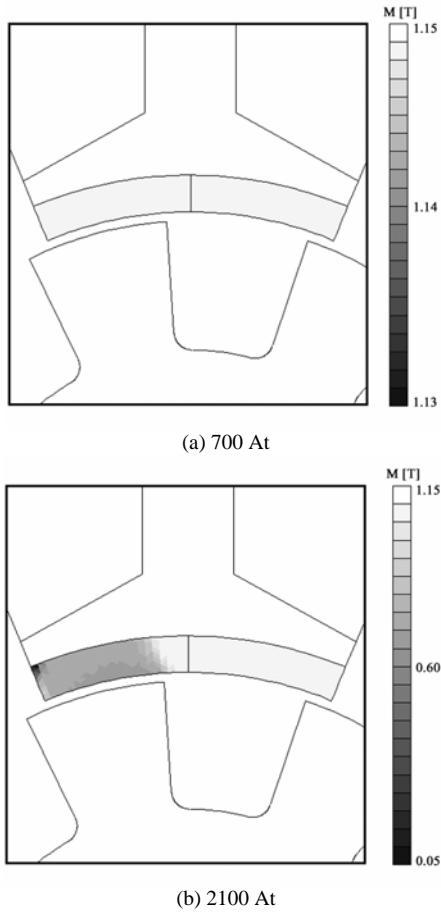

(a) 700 At

(b) 2100 At

Fig. 9. The magnetization distribution of the magnet.

(a) 700 At

(b) 2100 At
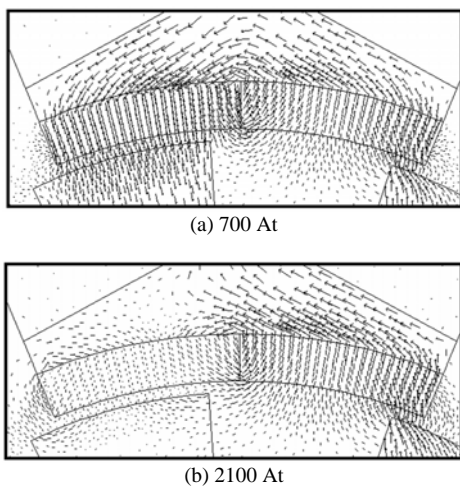
Fig. 10. Flux vectors according to MMF.

Fig. 11 compares the measured Back-EMF at 1500rpm when the magnet thickness is 2mm. From fig. 11, the Back-EMF is reduced when the MMF is 2100 Ampere-turns. This can be explained by the demagnetization. After all, the irreversible magnet demagnetization deteriorates the performance of a FRM.
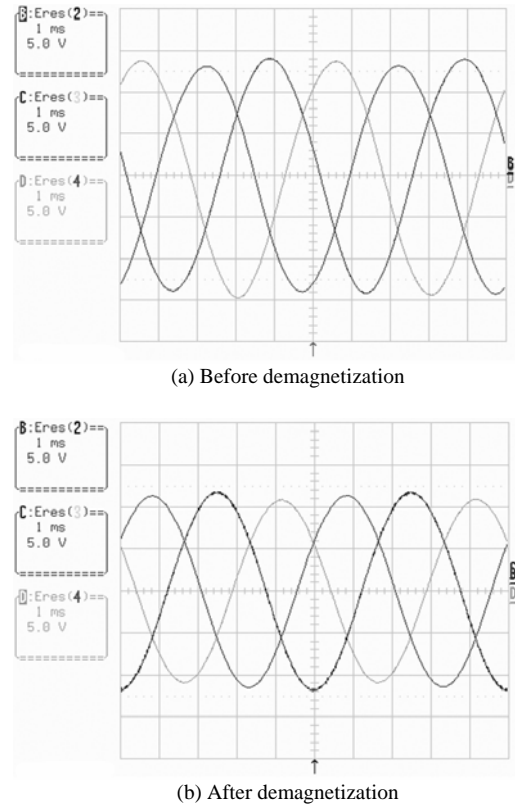

(a) Before demagnetization

(b) After demagnetization

Fig. 11. The measured Back-EMF.

V. CONCLUSION

In this paper, the irreversible magnet demagnetization analysis of a FRM has been studied both theoretically and experimentally. The nonlinear characteristic of the permanent magnet is considered as well as that of a magnetic core on each B-H curve. As a result, magnet thickness and rotor teeth width are the most important geometrical dimensions of a FRM in terms of irreversible magnet demagnetization. It is also shown that irreversible magnet demagnetization reduces the Back-EMF and deteriorates the performance of a FRM.

REFERENCES

[1] Deodhar. R. P., Andersson. S., Boldea. I., Miller. T. J. E., "The flux-reversal machine: a new brushless doubly-salient permanent-magnet machine", IEEE trans. on industry applications, Vol. 33, No. 4, pp. 925-934, 1997.

[2] Y. Liao, F. Liang, and T. A. Lipo, "A novel permanent-magnet motor with doubly-salient structure," IEEE Trans. Ind. Applica., vol. 31, pp. 1069-1078, Sept.-Oct. 1995.

[3] H. C. Lovatt and P. A. Watterson, "Energy Stored in Permanent Magnets," IEEE Trans. Magn., vol. 35, pp. 505-507, 1999.

[4] G. H. Kang, J. Hur, H. Nam, J. P. Hong, and G. T. Kim, "Analysis of irreversible magnet demagnetization in line-start motors based on the finite-element method," IEEE Trans. Magn., vol. 39, pp. 1488-1491, May 1999.

[5] S. J. Salon, Finite Element Analysis of Electrical Machines. Kluwer Academic Publishers, 1995.